Article:
Ghanbarzadeh, A, Wilson, M, Morina, A et al. (2016) Development of a new mechano-chemical model in boundary lubrication. Tribology International, 93 (Part B). pp. 573-582. ISSN: 0301-679X

https://doi.org/10.1016/j.triboint.2014.12.018

Development of a New Mechano-Chemical Model in Boundary Lubrication

Leeds/Lyon Conference, Sept, 2014

Ali Ghanbarzadeh, Mark Wilson, Ardian Morina, Duncan Dowson, Anne Neville

Institute of Functional Surfaces (IFS) , University of Leeds, Leeds, LS2 9JT

E-mail:mnag@leeds.ac.uk

Keywords: Boundary lubrication, Tribochemistry, Contact mechanics

Abstract

A newly developed tribochemical model based on thermodynamics of interfaces and kinetics of tribochemical reactions is implemented in a contact mechanics simulation and the results are validated against experimental results. The model considers both mechanical and thermal activation of tribochemical reactions instead of former thermal activation theories. The model considers tribofilm removal and is able to capture the tribofilm behaviour during the experiment. The aim of this work is to implement tribochemistry into deterministic modelling of boundary lubrication and study the effect of tribofilms in reducing friction or wear. A new contact mechanics model considering normal and tangential forces in boundary lubrication is developed for two real rough steel surfaces. The model is developed for real tribological systems and is flexible to different laboratory experiments. Tribochemistry (e.g. tribofilm formation and removal) and also mechanical properties are considered in this model. The amount of wear is calculated using a modified Archard's wear equation accounting for local tribofilm thickness and its mechanical properties. This model can be used for monitoring the tribofilm growth on rough surfaces and also the real time surface roughness as well as changes in the λ ratio. This model enables the observation of *in-situ* tribofilm thickness and surface coverage and helps in better understanding the real mechanisms of wear.

Nomenclature

Parameter	Description	Parameter	Description
p	Normal pressure (Pa)	C_1, C_2, A_1	Tribofilm formation constants
V^*	Complementary potential energy (J)	E_f^*	Tribofilm elastic modulus (Pa)
$\bar{u}_z, u_x, u_y, u_z$	Surface deformations (m)	$E_{0_f}^*$	Threshold elastic modulus (Pa)
$\bar{u}_z^*$	Surfaces prescribed deformation (m)	H_0	Tribofilm threshold hardness (Pa)
E_1, E_2, E^*, G^*	Elastic and shear modulus (Pa)	H	Tribofilm hardness (Pa)
q, q_x, q_y	Tangential pressure (Pa)	K	Dimensionless Archard wear constant
v_1, v_2	Poison ratio	COW_{tr}	Archard's wear coefficient for tribofilm
C_{kl}	Coefficient matrices	COW_{steel}	Archard's wear coefficient for steel
a, b	Discretised area length (m)	COW_{min}	Archard's wear coefficient for steady state tribofilm
t	Time (s)		
$k_{tribo-thermo}$	Tribochemical reaction rate constant (s^{-1})		
k_{thermo}	Thermal reaction rate constant (s^{-1})		
x_{tribo}	Tribo-activation reaction factor		
x_{thermo}	Thermal activation reaction factor		
k_1	Boltzmann constant ($m^2 kgs^{-2}k^{-1}$)		
T	Temperature (k)		
h'	Planck's constant ($m^2 kgs^{-1}$)		
ΔE	Activation energy (J)		
R	Gas universal constant ($Jmolk^{-1}$)		
A, B, C	Chemical concentrations (mol)		
h_{max}	Maximum film thickness due to formation		
h	Tribofilm thickness		
C_3, C_4	Removal constants		

1. Introduction

Boundary lubrication is the lubrication regime where the interface behaviour is dominated by chemical reactions that happen at the surfaces, tribofilm formation occurs, and the load is carried by the asperities. In the boundary lubrication regime the asperity-to-asperity contacts (Figure 1) may lead to elastic or plastic deformation or even fracture and can generate frictional heat which will be accompanied by chemical reactions to produce organic and inorganic surface films. A wide range of studies regarding many aspects of tribofilm formation and removal and their roles in reducing friction and wear have been conducted [1,2].

The effectiveness of boundary lubrication has been considered for a long time as a necessity for modern designs of machines with reliable operations. Because of the need for more energy efficiency, availability of new materials and machine part downsizing, the need for understanding true interactions in this regime is of great importance. The boundary lubrication regime has been the subject of many studies for more than 70 years [3,4] and the majority of these studies are experimental investigations into the nature of what happens in this regime. Many of the studies cover the boundary film chemical [5,6], physical and mechanical properties [7-11] and their effects on wear and friction reduction. The subject of many works has been to investigate different kinds of additives in oils and their effects on various aspects of tribological performance [1,2,12]. As the boundary lubrication regime is mainly related to interactions of two surfaces and the additive containing oils between them, the analytical studies of surfaces including topography measurements, chemical analyses, mechanical and physical studies are considerable. All these experiments give good insight into different chemical and physical characteristics covering various aspects of boundary lubrication systems.

It is clear from the wealth of experimental literature in this area that the nature of the phenomena happening in this regime is very complicated. Studying the entire problem needs a multiscale understanding ranging from component scale down to the micro-scale and also molecular interactions of films and lubricant additives. Experimentation across such scales is challenging and hence it is important to complement such studies with the ability to predict the friction and wear of a working system without running experiments. It is also important to analyse the system and optimise its performance in order to design cost effective experiments. Many modelling attempts have been made in the past years but a comprehensive

multiscale model of boundary lubrication considering tribochemistry phenomena in order to predict friction and wear of the system is still lacking.

Sullivan [13] developed a model for oxidational wear under boundary lubrication. He proposed a mathematical model which relates the wear to applied load and pressure and involves many other factors that together can be assumed as Archard's wear equation coefficient. However there is no detailed contact mechanics in this model. Stolarski [14] developed a model for wear prediction in boundary lubricated contacts both in dry and lubricated contact between sliding surfaces. He used statistical models and probability functions to predict the asperity-asperity contact, determining the probability of elastic or plastic contact and thus calculating the wear. That approach used the Greenwood and Williamson model of contact mechanics [15]. Zhang et al [16] derived a model for micro contacts. The deformation of asperities in this model can be elastic, elasto-plastic or even fully plastic and the possibility of contacts are determined by a contact probability equation. They used the Jaeger equation [17] over the contact area in order to calculate the asperity flash temperature. Classical wear theories were used for calculating the probability of contact covered by oxide layer and also probability of contact covered by physically and chemically adsorbed layers were studied.

Recently, Bosman *et al*. [18] proposed a numerical model for mild wear prediction under boundary lubrication systems. They assumed that the main mechanisms that protect the boundary lubricated system are the chemically reacted layers and when these layers are worn off, the system will restore the balance and the substrate will react with the oil to produce a tribofilm. They also proposed a transition from mild wear to more severe wear by making a complete wear map. Hegadekatte *et al*. [19] developed a multi-time-scale model for wear prediction. They used commercial codes for determining their contact pressure and deformations and then used Archard's wear equation for calculating wear. Anderson *et al.* [20] used a wear model and implemented FFT based contact mechanics simulations to calculate contact pressure and deformations.

Another recent work by Anderson *et al.* [21] used contact mechanics of rough surfaces considering the tribofilm properties and also the tribofilm formation and growth. They used an Arrhenius equation for the tribofilm growth and Archard's wear equation for wear predictions. The novelty of this work was considering the tribofilm and also film formation rate during the time. The film formation was following an exponential formulation based on

Arrhenius equation. The model was based on contact pressure and flash temperature and these parameters were responsible for tribofilm growth. They calibrated their tribofilm equation at the local scale and calculated the average tribofilm at the global scale. The model considered the tribofilm thickness and the hardness variation through the film but did not consider the elastic properties of the tribofilm. They used a simple form of Archard's wear equation and calibrated the equation based on experimental results. The work presented here was considered as a modification to that work but there are several improvements in this model that are highlighted in the paper.

Despite the important role tribochemistry plays in the behaviour of tribosystems, there is no comprehensive modelling framework that considers tribochemistry in boundary lubrication. The main aim of this work is therefore to build such a framework to implement tribochemistry into boundary lubrication modelling that can predict friction and wear of the system with respect to the effect of the tribofilm.

The importance of tribofilms and an attempt to find the true mechanisms involved in reducing wear and friction will be studied in this work. The model was built in a way that it would be flexible for various working conditions and different real tribosystems as well as different additives and their concentrations.

2. Components of the model

To study the contact of real rough surfaces, digitized rough surfaces are important inputs of all numerical studies. These digitized surfaces can be either generated mathematically or can be obtained from surface measurement instruments like Atomic Force Microscope.

In this work rough surfaces are generated using the method proposed by Tonder *et al.* [22] using digital filters. These two rough surfaces are in contact with each other and the results are contact pressures and surface deformation in interfaces.

The main components of the model are contact mechanics, tribofilm model and wear which are now discussed.

2.1. Contact Mechanics

There have been many attempts at simulating the contact of rough surfaces in contact mechanics [23-35]. The contact mechanics model developed by Tian and Bhushan [36] which considers the complementary potential energy will be used in this work. By applying

the Boussinesq method and relating the contact pressures to surface deformations, the problem would be to solve the contact mechanics only for finding contact pressures at each node and then the related contact deformations can be calculated. For this model, surfaces should be discretised into small nodes and it is assumed that the nodes are small enough and the contact pressure is constant at each node.

The problem is to minimize the complementary potential energy as follows:

$$V^* = \frac{1}{2}\iint p\overline{u_z}\,dxdy - \iint p\,\overline{u_z^*}\,dxdy \qquad (1)$$

where p is the contact pressure and V^*, $\overline{u_z}$ and $\overline{u_z^*}$ are complementary potential energy, surface deformation and prescribed displacement respectively.

The Boussinesq solution for relating contact pressure and surface deformation usually considers only normal forces and the solution is:

$$u(x_1, x_2) = \frac{1}{\pi E^*}\iint_{-\infty}^{\infty} \frac{p(s_1, s_2)}{\sqrt{(x_1 - s_1)^2 + (x_2 - s_2)^2}} ds_1 ds_2 \qquad (2)$$

in which E^* is the composite elastic modulus of two surfaces. There are few works considering both normal forces and tangential forces and the majority of them use combined FEM and BEM to capture the effect of tangential forces on surface deformation.

The Basic Boundary Equation for the elastic half space is well known as:

$$u(x_1, x_2) = \frac{1}{\pi E^*}\iint_{-\infty}^{\infty} \frac{p(s_1,s_2)}{\sqrt{(x_1-s_1)^2+(x_2-s_2)^2}} ds_1 ds_2 + \frac{1}{\pi G^*}\iint_{-\infty}^{\infty} \frac{q(s_1,s_2)(x_1-s_1)}{(x_1-s_1)^2+(x_2-s_2)^2} ds_1 ds_2 \qquad (3)$$

This equation expresses the relation of u_z (surface deformation) with normal force and tangential force in one direction. In which, $E^*$and G^* are the composite Young's and shear modulus of the surfaces and are calculated from:

$$\frac{1}{E^*} = \frac{(1-{\nu_1}^2)}{E_1} + \frac{(1-{\nu_2}^2)}{E_2} \qquad (4)$$

$$\frac{1}{G^*} = \frac{(1+\nu_1)(1-2\nu_1)}{2E_1} - \frac{(1+\nu_2)(1-2\nu_2)}{2E_2} \qquad (5)$$

Here, ν_1, ν_2, E_1 and E_2 are the Poisson's ratio and Elastic Modulus of surfaces 1 and 2 respectively. In the equation (3), q is the tangential or shear load.

For solving the double integrals of equation (3) the surfaces should be discretised into small nodes. To solve the integral equation for the discretised surfaces the integral equations should be discretised first:

$$(\overline{u_z})_l = \frac{1}{\pi E^*}\iint \frac{p(x',y')dx'dy'}{\sqrt{(x'-x)^2+(y'-y)^2}} + \frac{1}{\pi G^*}\iint_{-\infty}^{\infty} \frac{q(s_1,s_2)(x_1-s_1)}{(x_1-s_1)^2+(x_2-s_2)^2} ds_1 ds_2 = \frac{1}{\pi E^*}\sum_{k=1}^{M}\iint \frac{dx'dy'}{\sqrt{(x'-x)^2+(y'-y)^2}} p_k + \frac{1}{\pi G^*}\sum_{k=1}^{M}\iint \frac{(x_1-s_1)}{(x_1-s_1)^2+(x_2-s_2)^2}\mu p_k = \sum_{k=1}^{M} C_{kl}p_k \quad (6)$$

It is assumed that the nodes are small enough for the pressure to be constant at the centre of each node. C_{kl} is the influence matrix and is calculated by solving the double integral:

$$C_{kl} = \frac{1}{\pi E^*}\iint_{-\infty}^{\infty} \frac{ds_1 ds_2}{\sqrt{(x_1-s_1)^2+(x_2-s_2)^2}} + \frac{\mu}{\pi G^*}\iint_{-\infty}^{\infty} \frac{(x_1-s_1)}{(x_1-s_1)^2+(x_2-s_2)^2} ds_1 ds_2 \quad (7)$$

The solution for the influence matrix in discretised form is as follows:

$$C_{kl} = \frac{1}{\pi E^*}\left\{(x+a)\ln\left[\frac{(y+b)+\sqrt{(y+b)^2+(x+a)^2}}{(y-b)+\sqrt{(y-b)^2+(x+a)^2}}\right] + (y+b)\ln\left[\frac{(x+a)+\sqrt{(y+b)^2+(x+a)^2}}{(x-a)+\sqrt{(y+b)^2+(x-a)^2}}\right] + (x-a)\ln\left[\frac{(y-b)+\sqrt{(y-b)^2+(x-a)^2}}{(y+b)+\sqrt{(y+b)^2+(x-a)^2}}\right] + (y-b)\ln\left[\frac{(x-a)+\sqrt{(y-b)^2+(x-a)^2}}{(x+a)+\sqrt{(y-b)^2+(x+a)^2}}\right]\right\} + \quad (8)$$

$$\frac{\mu}{\pi G^*}\Bigg\{(y+b)ln\left[\frac{\sqrt{(y+b)^2+(x+a)^2}}{\sqrt{(y+b)^2+(x-a)^2}}\right]+(y-b)ln\left[\frac{\sqrt{(y-b)^2+(x-a)^2}}{\sqrt{(y-b)^2+(x+a)^2}}\right]$$
$$+(x+a)\left[\tan^{-1}\frac{y+b}{x+a}-\tan^{-1}\frac{y-b}{x+a}\right]$$
$$+(x-a)\left[\tan^{-1}\frac{y-b}{x-a}-\tan^{-1}\frac{y+b}{x-a}\right]\Bigg\}$$

in which a and b are the half-length of each small node and μ is the coefficient of friction.

Equation (1) describes the potential energy for a frictionless contact and the normal force is the only force applied on the surfaces. The potential equation for a frictional contact would be modified to the form below:

$$V^* = \frac{1}{2}\iint t\,\bar{u}\,dxdy - \iint t\,\overline{u^*}\,dxdy \qquad (9)$$

In which t is the full surface pressure vector including the in-plane tractions and u is the full surface deformation.

$$t = q_x e_x + q_y e_y + p e_z \qquad (10)$$

$$u = u_x e_x + u_y e_y + u_z e_z \qquad (11)$$

q_x and q_y are the in-plane traction forces. Equations 3-8 are based on the assumption that $q_x = 0$ in the equation (10).

By applying the same discretising procedure, the Boussinesq solution for the fully coupled deformation-traction relationship can be expressed as:

$$u_{xk} = \sum_{l=1}^{M}\left(C_{kl}^{xx}q_{xl} + C_{kl}^{xy}q_{yl} + C_{kl}^{xz}p\right)$$
$$u_{yk} = \sum_{l=1}^{M}\left(C_{kl}^{yx}q_{xl} + C_{kl}^{yy}q_{yl} + C_{kl}^{yz}p\right) \qquad (12)$$
$$u_{zk} = \sum_{l=1}^{M}\left(C_{kl}^{zx}q_{xl} + C_{kl}^{zy}q_{yl} + C_{kl}^{zz}p\right)$$

In the matrix form:

$$\begin{bmatrix} u_x \\ u_y \\ u_z \end{bmatrix} = \begin{bmatrix} C^{xx} & C^{xy} & C^{xz} \\ C^{yx} & C^{yy} & C^{yz} \\ C^{zx} & C^{zy} & C^{zz} \end{bmatrix} \begin{bmatrix} q_x \\ q_y \\ p \end{bmatrix} \quad (13)$$

The elements of the influence matrix can be obtained from the complete solution of the Boussinesq problem. The solution for the above equation is mentioned in the appendix 1. Then the problem would be minimizing the potential energy for the fully coupled contact. The solution procedure is the same as frictionless contact and can be carried out by direct quadratic mathematical solution [36,55].

Solving the quadratic form of energy for 3D problem increases the computation time by several times and it has been examined by the authors that in the case of two similar materials it does not affect the true contact pressures significantly. Therefore the complementary potential solution was carried out only considering the normal load using the solution reported by Tian et al [36]. For the case of two identical materials in contact, the equivalent shear modulus of equation (5) becomes zero and the equation (3) reduces to equation (2). As the current study considers the contact of two similar materials, only the equation (2) and the discretized form of that equation which is the first part of equation (8) have been used for this first analysis.

It is assumed that two rough surfaces come into contact; one of the surfaces enters the contact with the other surface from one side and exits the contact on the opposite side (Figure 2). Both surfaces have speed and their speed difference depends on the slide-roll ratio of the systems. This process of two rough surfaces coming into contact is repeated to the end of the simulation. Therefore a rolling sliding motion can be easily modelled by this contact mechanics simulation. It should be noted that the contact mechanics model in this work is quasi-static.

The model is developed for a rolling sliding ball on ring experiment and all the configurations corresponding to real tribosystems are embedded into the model. The flexibility of the model to be adapted to various experiments has been examined by the author and the comparison between different experiments such as reciprocating and rotary ball on disc would be studied in future work.

2.2. Tribofilm model development

Friction is an irreversible process due to energy dissipation at interfaces which is a non-equilibrium process and should be studied using non-equilibrium thermodynamics [37-42].

Many results show that not only the flash temperature but also the entropy changes at interfaces are very important in tribochemical reactions. Hence the tribochemical reaction and the tribochemical film growth models should consider entropy and the factors affecting the entropy of the system. The concept of thermodynamics in the tribosystems has been the subject of many recent studies. There are some attempts to model tribofilm growth based on temperature dependency of tribochemical reactions [21] and also diffusion-reaction mechanisms [54]. Attempts were made to relate tribochemical reactions to non-equilibrium thermodynamics and changes in the entropy of the system.

It has been reported that the mechanical stress can play a significant role in inducing the tribochemical reactions. It is assumed that tribochemical reactions follow reaction theory but these reactions are activated not only by temperature but also by mechanical rubbing [43, 44, 56]. The current model is developed in a way that considers flash temperature as a parameter responsible for the formation but more importantly is the term x_{tribo} which is responsible for the mechanical activation of chemical compounds.

The proposed model is based on the Bulgarevich *et al.* [43,44] studies of tribochemical reactions. They used active collision theory and activated complex theory to describe the tribochemical reactions occurring in boundary lubrication. They stated that the induction force for the tribochemical reactions is mainly the mechanical rubbing or in other words the entropy change at interfaces not only the temperature. Therefore they suggested a formulation for rate of the reaction which is as follows:

$$k_{tribo-thermo} = \frac{x_{tribo}}{x_{thermo}} k_{thermo} \qquad (14)$$

$$k_{thermo} = \frac{k_1 T}{h'} exp\left(\frac{\Delta E}{RT}\right) \qquad (15)$$

$$x_{thermo} = exp\left(\frac{\Delta E}{RT}\right) \qquad (16)$$

Here, x_{tribo} and x_{thermo} are the effects of mechanoactivation and thermoactivation respectively. The terms x_{tribo} and x_{thermo} can be interpreted as the role of mechanoactivation and thermoactivation in inducing the tribochemical reactions. k_1 and h' are the Boltzmann and Plank's constant and ΔE, R and T are activation energy, gas universal constant and the temperature respectively. By substituting expressions for k_{thermo} and x_{thermo} into equation (14) the tribochemical reaction rate follows equation (17):

$$k_{tribo-thermo} = \frac{k_1 T}{h'} x_{tribo} \qquad (17)$$

The model in this work assumes that the tribofilm is a product of reaction between substrate and lubricant additives. It has been reported in the literature that the nature of such reactions are complicated [57, 58]. Because of this complexity, there is no clear picture of order of tribochemical reactions. It was assumed that the reaction is following a second order form and the results can be validated against experiments.

Here it is assumed that if the substance A (e.g. lubricant additive) and substance B (e.g. steel surface) form the substance C (e.g. tribofilm) due to tribochemical reaction, the reaction rate can be expressed as:

$$\frac{dC}{dt} = k_{tribo-thermo}\, A.B \qquad (18)$$

In which A, B and C are the concentrations of substances A, B and C. It is assumed that the substance B is sufficient for the chemical reactions and only substance A is limiting the rate of reaction. When the tribofilm becomes thicker it will limit the tribochemical reaction due to limiting the amount of nascent surface for forming a tribofilm. Therefore by assuming a maximum film thickness for the tribofilm the dependence of substance A on the tribofilm thickness can be expressed as:

$$A = A_1(h_{max} - h) \qquad (19)$$

By substituting equations (17,19) into equation (18) , the tribochemical reaction rate becomes:

$$\frac{dC}{dt} = k_{tribo-thermo}\, A_1(h_{max} - h)\, B$$

$$\frac{dC}{dt} = \frac{k_1 T}{h'} x_{tribo}\, .C_1.(h_{max} - h) \qquad (20)$$

In this equation C_1 is A_1B. The tribochemical reaction rate can be related to film thickness by using a relation constant as bellow:

$$\frac{dh}{dt} = \frac{k_1 T}{h'} x_{tribo} \,.\, C_2 .\, (h_{max} - h) \qquad (21)$$

Here C_2 includes C_1 and another constant.

By integrating this equation, the tribofilm thickness as a function of time can be given by:

$$h = h_{max}(1 - e^{\left(-\frac{k_1 T}{h'} . x_{tribo} . t\right)}) \qquad (22)$$

It is noticeable that this equation is similar to Spike's proposed model for ZDDP tribofilm growth based on the reported experimental results [45].

The difference between this model and other attempts for capturing tribofilm growth is the ability to have local properties of surfaces.

The temperature used in this model is the temperature at asperities which is the summation of flash temperature and bulk temperature [46]. The Jaeger's moving heat source analysis is used in this work and the flash temperature is calculated for the square heating area. The term x_{tribo} is an indication of entropy change in the system due to mechanical rubbing. This term will be different for different applications and lubricant-substrate combinations and modifies the Arrhenius equation in a way that effect of mechanical activation of chemical compounds is being considered. It was reported by Bulgarevich et al [43, 44] that population of transition states of activated complex due to mechanical rubbing is much more than the thermal activated ones for the tribochemical reactions. They proposed simple formulations for the term x_{tribo} for a single asperity- asperity contact. The aim of the proposed model in this work was to adapt this model to the large scale observations of tribosystems in order to enable this term to be defined based on experimental results. Therefore, the model is semi-analytical and the term x_{tribo} can be calibrated from the in-situ tribofilm thickness measurements although it has the meaning as explained above. This term is responsible for the mechanical activation of the reactants and also rubbing effect on formation of the tribofilm. It can be a starting point to model tribofilm kinetics based on different parameters affecting the growth. The authors are currently investigating the effect of different parameters such as additive concentration on the term x_{tribo}.

A thorough investigation of the term x_{tribo} for different systems is currently underway and will be reported in due course. Here the model is illustrated for ZDDP additive in base oil for the rubbing of steel on steel surfaces.

The effect of tribofilm removal must also be considered in the model; it is assumed that the tribofilm both grows and is also partially removed in each time step. The wear model described in section 2.4 represents how the presence of a tribofilm modifies the local wear of the substrate. However the model does not predict the removal of the tribofilm itself.

The authors suggest that the tribofilm is being removed and formed at the same time. The process of formation and removal of the tribofilm in combination, will lead to growth of the film on the substrate. It was also reported by Lin et al [59] that the tribofilm is formed and removed at the same time and the balance between the rate of formation and removal explains the behaviour of the system. A wide ranging of literature search suggests that a removal model was reported by Fujita-Spikes in [12]. In that work the removal was studied and an exponential form was proposed for the removal terms. The versatile exponential form of the removal occurs. The authors have tested different functions for capturing the whole behaviour of the tribofilm and the exponential one seems to cover the behaviour in all reported experimental cases. At this early stage there is no clear picture of the dominant removal process from the initial experiments. In the future work, authors intend to develop this model and use the numerical framework to investigate the effect of different parameters in the removal of the tribofilm. Removal plays an important role in the behaviour of tribosystems and the current model offers an insight into the removal processes and how these relate to wear of the system.

Assuming that tribofilm removal also follows an exponential form, equation (23) is to

$$h = h_{max}\left(1 - e^{\left(-\frac{k_1 T}{h'}.x_{tribo}.t\right)}\right) - C_3(1 - e^{-C_4 t}) \quad (23)$$

in which $C_3$and C_4 are removal constants. These removal terms were calibrated with experimental results and have been reported in table (1). It is shown in the figure (4) that the model fits well with the experimental data. The single points are the Spacer Layer Interferometry Method (SLIM) tribofilm thickness results and the line is the fitted model. The

fitting accuracy is shown in the figure (4) and the factors indicating the goodness of the fitting is included in the table (1).

The comparison between tribofilm removal and substrate wear, and the ability to isolate each, can help to understand better the true mechanisms of wear. This investigation can help tribologists to relate tribofilm removal to wear of the system. The model is able to calculate tribofilm removal at any time steps and can help to monitor removal during the time. It can be used to compare tribofilm formation and removal rate at any time of the tribosystems runs. Studying the effect of different parameters on tribofilm removal can be carried out in this model which might be a starting point to model film removal based on different factors.

This is the first attempt to fully capture the tribofilm growth (both formation and removal) in local scale which enables us to monitor the growth on global scale. The previous attempt by Andersson et al [21] showed a good behaviour for predicting tribofilm formation. The tribofilm removal was not considered in that work which is of great importance as suggested by the authors of the current article.

The inhomogeneity of tribological systems has been considered with a great importance in the current work. The roughness of the surfaces will lead to inhomogeneous distribution of load and also temperature on the surfaces which will consequently result in different film formation and removal at different parts of the surfaces. It is directly implemented into the nature of the model that the tribofilm forms differently on different areas in the surface. This inhomogeneity in the local properties of rough surfaces will result in different wear behaviours.

2.3. Tribofilm properties

There are several works which study the mechanical properties of tribofilms formed in boundary lubricated contacts and many techniques are used to understand what behaviours lead to these properties [7-11]. They found that the properties of the tribofilm layers are dependent on applied loads and can be adapted to conditions. They also showed that the mechanical properties of tribofilms vary from surface to substrate.

Mosey et al [47] developed a new theory for the functionality of ZDDP tribofilms at the molecular level. They suggested that pressure induced cross-linking is the reason for chemically connected networks and many experimentally validated behaviours of ZDDP can be explained by this theory. It was reported that the high pressure at the surface of the film

will lead to higher cross-linking and result in longer chain phosphates. The different mechanical properties of high and short chain polyphosphates were also reported in the work. The effect of the steel substrate in changing the nano-indentation results of tribofilm has been reported and different models for extracting the tribofilm properties were developed [7,48]. In this work the results reported for the mechanical properties of tribofilm based on those models has been used.

Demmou et al [48] found that the pressure affects the elastic properties of the tribofilm and it will happen when the pressure exceeds a threshold amount of H_0. So for contact pressures below H_0 the elastic modulus is constant and after that it will change by variation of hardness. The linear function of this relation is given below:

$$E_f^* = \frac{E_{f_0}^*}{H_0} H \qquad (24)$$

E_f^* is the film reduced modulus and $E_{f_0}^*$ is the constant elastic modulus before threshold pressure. $E_{f_0}^*$ was almost the same for all temperatures and equal to 39 ± 4GPa. H_0 was found to be dependent on temperature.

In summary, the assumptions for the mechanical properties of the tribofilm are based on previous studies of ZDDP or ZDDP/MoDTC tribofilms properties. ZDDP tribofilms have a thickness of 50-150nm and the mechanical properties change from the surface to the bulk. The hardness at the surface is lower than the bulk hardness; as the penetration depth increases the hardness increases linearly [48,49].

The value of surface tribofilm hardness and tribofilm hardness near the substrate can be obtained from experimental results but the variations can be assumed to be between 2 to 6 GPa. In addition, elastic properties of the tribofilm also vary from the surface to the bulk and this variation is related to hardness variation of tribofilm as previously explained.

Because of the limitations in the half space theory and the Boussinesq solution, implementation of varied elastic modulus for different local points is very complicated. Therefore a way of considering different elastic modulus value for different local points on the surface was suggested here in this work. The elastic modulus is the average of modulus of all local points on the surface and the amount is used in the Boussinesq formulation.

Considering the plastic deformation, a mathematical formulation should be used in order to consider the tribofilm hardness variations when the tribofilm deforms plastically. This model considers the two surfaces and their deformations and shows how the hardness is calculated in different deformation conditions. The model was developed by Andersson et.al [21] and a similar formulation but different procedure is used in this work. In the initial model a linear variation of hardness value from surface to bulk of the tribofilm have been considered. The tribofilm contributes to changes to the hardness of the layer because of its thickness. This hardness contributes to the elastic-plastic contact model and gives the plastic deformation in the system. The height of the tribofilm always follows the growth behaviour of the tribofilm in real systems and it changes both the hardness of local asperities and the plastic behaviour of the system.

2.4. Wear modelling

A modified version of Archard's wear equation [50] was used in this work. When the contact pressures are calculated, it is a straightforward procedure to calculate the wear depth. The sliding speed and the time scale should be considered in implementing the wear equation. The pressure is assumed to be constant in each time step and the wear is calculated by Archard's equation for each single asperity.

So the resulting wear depth of the surfaces during each time step is calculated as:

$$\Delta h(x,y) = \frac{K}{H}.P(x,y).\Delta t.v \qquad (25)$$

in which H , K, P and v are the material hardness, dimensionless Archard's coefficient, local contact pressure and sliding speed respectively.

The above equation will be computed at every time step and the pressure distributions are the pressures calculated at each time steps from contact mechanics simulations.

All the parameters in the above equation are calculated in the contact mechanics simulation except Archard's wear coefficient (K). An assumption is made in this work in order to consider the effect of the tribofilm in reducing wear by relating the wear coefficient to the thickness of the tribofilm. It has been proved that some additives such as ZDDP reduce wear significantly but the real mechanism of this wear reduction is still missing and is the subject

of many researches. In this work a way to study the effect of ZDDP tribofilm in reducing wear is proposed. It is assumed that in the areas where tribofilm is formed, the coefficient of wear is less than the areas where tribofilm is not formed. The coefficient of wear is assumed to change linearly with tribofilm height.

Assuming that the coefficient of wear is at its maximum for steel-steel contact and at its minimum when the tribofilm has its maximum thickness, the equation for calculating coefficient of wear is as follows:

$$CoW_{tr} = CoW_{steel} - (CoW_{steel} - CoW_{min}).\frac{h}{h_{max}} \qquad (26)$$

The relationship can be clearly seen in figure 3. CoW_{tr} is the coefficient of wear for tribofilm with thickness h.

CoW_{steel} , CoW_{min} and h_{max} are coefficient of wear for steel and coefficient of wear corresponding to maximum ZDDP tribofilm thickness and maximum film thickness respectively.

It can be seen from the formulation above that the tribofilm can affect the wear when it is formed on the surface. Also the growth of tribofilm both in thickness and coverage can affect the wear significantly. The wear considered in this work is the mild wear which occurs due to the chemical reactions between steel substrate and the lubricant additives. In the process of tribofilm formation and removal, the substrate should react with the lubricant additives to form the tribofilm. Therefore the substrate can be worn in presence of the tribofilm which is being observed in experimental findings.

3. Numerical implementation

Based on experimental observations, it is assumed that the tribofilm is formed only on the asperities that are in contact. The contact mechanics simulation gives the local properties of rough surfaces and these properties are fed into the tribofilm development model to calculated local tribofilm growth. The local calculated film is put on top of the initial surface and the amount of wear is calculated using the modified Archard's equation discussed above. The geometries of the rough surfaces are changed due to plastic deformation and wear as well as the local tribofilm growth. In the simulation, the amount of wear and plastic deformation is subtracted from the substrate geometry itself not from the tribofilm. The tribofilm is only following the tribofilm growth model and is not affected by wear. The reason for this

assumption is that, tribofilm removal is being considered as a separate factor in this work. In addition, the real physics of wear of materials results in the assumption that wear should be considered as the material (substrate) loss. This procedure is continued as a loop till the end of simulation. The area of study was a 20µm×20µm area at the middle of the wear track.

4. Model calibration

The developed model is based on deterministic contact mechanics and includes Archard's wear equation and also a developed model for tribofilm formation. Therefore the model needs to be calibrated for both Archard's wear coefficient and also tribofilm growth formulation. The experimental results used are from the thesis of Naveira Suarez [51]. The experiments are rolling sliding for ball on ring. The ball is steel 52100 with diameter and $R_a$value of 20mm and 10nm respectively. The ring is also steel 52100 and the R_a value is 100nm. Tribofilm thickness results for different slide to roll ratios have been used to calibrate the tribochemical model. The model calibrated for the maximum Hertzian pressure of 1.9 GPa is shown in this work as well as some predictive results.

In order to calibrate the model the experiment configuration should be considered in the contact mechanics simulations. Therefore two small surfaces of 20µm×20µm were in contact and the rolling-sliding motion was simulated for surfaces in the way that surfaces are moved due to their speeds and one surface is moving faster than another surface depending on the SRR.

The calibrated parameters are shown in table (1).

Table 1 Calibrated parameters from experiments and used in simulation

5. Results

The results are for a ball on ring rolling-sliding contact for an entraining speed of 0.25 m/s and average Hertzian contact pressure of 1.26 MPa. The oil used in the experiments was PAO with 2.5% ZDDP. The SRR is 5% and the ball and ring properties are the same as those used for calibration.

5.1. Tribofilm local growth

Figure 4 shows the calibrated tribofilm growth results from the simulation. It shows the tribofilm thickness results based on the calibrated parameters listed in table1. It can be seen

that the ZDDP tribofilm is forming on the surface and the thickness is increasing with time. Also the tribofilm is covering the surface and the coverage is increasing with time and this coverage interpretations can be found in simulations results but is not presented in this paper . The maximum tribofilm thickness is plotted as well as the results from Naveira Suarez's thesis and an agreement can be seen. The experimental results are tribofilm average thickness measurements carried out by Spacer Layer Imaging Method. The in situ average tribofilm thickness measured in this method was used to calibrate the model and also used for comparison. The local tribofilm thickness was used to calibrate the model. In addition average film thickness which is the average tribofilm thicknesses of all local points, is plotted for different slide to roll ratios in figure 5. It can be seen that the local tribofilm growth model captures well the global tribofilm formation. This is the first time that a local tribochemical model can monitor the growth (formation and also removal) of tribofilm on global scale.

5.2. Wear calculations

The amount of total wear can be calculated by summation of wear of all local points. Wear calculation is plotted against time (figure 6) and it can be seen that wear rate at the beginning of the experiment is much more than the rate after running in. The difference between these wear rates can be interpreted as the effect of ZDDP tribofilm formation in reducing wear. It can also help to distinguish between running in and steady state wear. It is clear from the assumptions in the model, that the more the tribofilm grows the more the surface is protected from wear. By comparing the tribofilm growth with the wear during the simulation, it can be seen that the thicker tribofilm can result in a lower wear rate.

The wear calculation pattern in this work shows a good agreement with experimental results and also numerical predictions reported in the literature [19,52-54]. It allows the consideration of tribochemistry in predictive wear modelling and hence the investigation of the effect of different lubricant additives in reducing wear or even friction.

5.3. Surface roughness variations

Surface roughness changes during the tribological system runs due to different factors such as plastic deformation, wear of material and also tribofilm formation. Monitoring the surface roughness variation during the experiments is very difficult, yet it is also very important for machine element designers to know the surface roughness variations during real system runs. Also understanding the true mechanisms involving in surface roughness changes can help designers to prevent catastrophic damage to the machine elements and optimize their designs.

Study of the roughness has been the subject of many works to better understand the running in process and can help to link surface geometry changes to tribological performance of systems during running-in. Variation of the R_a value can be monitored using the developed model and also different factors affecting the R_a value (such as plastic deformation and wear of materials) can be monitored during the simulation. An example of the surface roughness variations is shown in the figure 7. The results are for the simulations based on the model calibrated above. It can be seen that the roughness change is dramatic at the beginning of the contact which is because of the plastic deformations in the beginning. The roughness continues to decrease because of the mild wear. This decrease pattern is only for the rougher surface and the smooth surface experiences a different pattern. These roughness variations are very dependent on roughness of the both surfaces and changing one of the surfaces can result in a different pattern of roughness variations for both surfaces.

Conclusions

A newly developed model for boundary lubrication in real tribosystems has been developed. This model considers tribochemistry and its effects on wear as well as mechanical properties of surfaces. Local tribofilm growth considering both formation and removal can be calculated in this model and it is possible to monitor the global tribofilm formation on the surfaces. It was shown that the global average tribofilm thickness shows a very similar trend to macroscale experimental studies of tribofilm growth. It therefore represents a good start in implementing tribochemistry into predictive boundary lubrication models. The tribofilm removal model can help tribologists to compare tribofilm removal with amount of wear and will give a good insight for real mechanisms of wear.

The effect of this tribofilm on local wear of the system is being considered and this can lead to a robust framework for predicting wear in boundary lubricated contacts. The model is applicable to a wide range of experimental observations and is able to be adapted to different experimental configurations.

The surface roughness variations with time can be calculated in this model which is of great importance for machine element designers. The tribofilm formation model includes a term, x_{tribo}, for the entropy change of the system. The effects of roughness and load on the term x_{tribo} need to be studied in detail, and this is the subject of current ongoing work. Further predictive results will be published in the near future.

6. Acknowledgement

This study was funded by the FP7 program through the Marie Curie Initial Training Network (MC-ITN) entitled “ENTICE - Engineering Tribochemistry and Interfaces with a Focus on the Internal Combustion Engine” [290077] and was carried out at University of Leeds. The authors would like to thank to all ENTICE partners whom had kind discussions on the topic and the methodology.

7. References.

- [1] Studt, P. "Boundary lubrication: adsorption of oil additives on steel and ceramic surfaces and its influence on friction and wear." *Tribology international* 22.2 (1989): 111-119

- [2] Morina, A., & Neville, A. (2007). Tribofilms: aspects of formation, stability and removal. Journal of Physics D: Applied Physics, 40(18), 5476.

- [3] Beeck, O., Givens, J. W., & Williams, E. C. (1940). On the mechanism of boundary lubrication. II. Wear prevention by addition agents. Proceedings of the Royal Society of London. Series A. Mathematical and Physical Sciences, 177(968), 103-118.

- [4] Tonck, A. J. M. P. H. J. M., Martin, J. M., Kapsa, P., & Georges, J. M. (1979). Boundary lubrication with anti-wear additives: study of interface film formation by electrical contact resistance. Tribology international, 12(5), 209-213.

- [5] Martin, J. M., Onodera, T., Minfray, C., Dassenoy, F., & Miyamoto, A. (2012). The origin of anti-wear chemistry of ZDDP. Faraday discussions, 156, 311-323.

- [6] Pawlak, Z. (2003). Tribochemistry of lubricating oils (Vol. 45). Elsevier.

- [7] Bec, S., Tonck, A., Georges, J. M., Coy, R. C., Bell, J. C., & Roper, G. W. (1999). Relationship between mechanical properties and structures of zinc dithiophosphate anti–wear films. Proceedings of the Royal Society of London. Series A: Mathematical, Physical and Engineering Sciences, 455(1992), 4181-4203.

- [8] Nehme, G., Mourhatch, R., & Aswath, P. B. (2010). Effect of contact load and lubricant volume on the properties of tribofilms formed under boundary lubrication in a fully formulated oil under extreme load conditions. Wear, 268(9), 1129-1147.

- [9] Aktary, M., McDermott, M. T., & McAlpine, G. A. (2002). Morphology and nanomechanical properties of ZDDP antiwear films as a function of tribological contact time. Tribology letters, 12(3), 155-162.

- [10] Nicholls, M. A., Do, T., Norton, P. R., Kasrai, M., & Bancroft, G. M. (2005). Review of the lubrication of metallic surfaces by zinc dialkyl-dithiophosphates. Tribology International, 38(1), 15-39.

- [11] Mourhatch, R., & Aswath, P. B. (2011). Tribological behavior and nature of tribofilms generated from fluorinated ZDDP in comparison to ZDDP under extreme pressure conditions—Part II: Morphology and nanoscale properties of tribofilms. Tribology International, 44(3), 201-210..

- [12] Morina, A., & Neville, A. (2007). Understanding the composition and low friction tribofilm formation/removal in boundary lubrication. Tribology International, 40(10), 1696-1704.

- [13] Sullivan, J. L. (1986). Boundary lubrication and oxidational wear. Journal of Physics D: Applied Physics, 19(10), 1999..

- [14] Stolarski, T. A. (1996). A system for wear prediction in lubricated sliding contacts. Lubrication science, 8(4), 315-351..

- [15] Greenwood, J. A., & Williamson, J. B. P. (1966). Contact of nominally flat surfaces. Proceedings of the Royal Society of London. Series A. Mathematical and Physical Sciences, 295(1442), 300-319..

- [16] Zhang, H., Chang, L., Webster, M. N., & Jackson, A. (2003). A micro-contact model for boundary lubrication with lubricant/surface physiochemistry. Journal of tribology, 125(1), 8-15.

- [17] Carslaw, H. S., & Jaeger, J. C. (1959). Heat in solids (Vol. 19591). Clarendon Press, Oxford.

- [18] Bosman, R., & Schipper, D. J. (2011). Mild wear prediction of boundary-lubricated contacts. Tribology letters, 42(2), 169-178..

- [19] Hegadekatte, V., Hilgert, J., Kraft, O., & Huber, N. (2010). Multi time scale simulations for wear prediction in micro-gears. Wear, 268(1), 316-324..

- [20] Andersson, J., Almqvist, A., & Larsson, R. (2011). Numerical simulation of a wear experiment. Wear, 271(11), 2947-2952.

- [21] Andersson, J., Larsson, R., Almqvist, A., Grahn, M., & Minami, I. (2012). Semi-deterministic chemo-mechanical model of boundary lubrication. Faraday discussions, 156(1), 343-360.

- [22] Hu, Y. Z., & Tonder, K. (1992). Simulation of 3-D random rough surface by 2-D digital filter and Fourier analysis. International Journal of Machine Tools and Manufacture, 32(1), 83-90..

- [23] Almqvist, A., Sahlin, F., Larsson, R., & Glavatskih, S. (2007). On the dry elasto-plastic contact of nominally flat surfaces. Tribology international, 40(4), 574-579..

- [24] Thompson, R. A., & Bocchi, W. (1972). A model for asperity load sharing in lubricated contacts. ASLE TRANSACTIONS, 15(1), 67-79..

- [25] Bhushan, B. (1998). Contact mechanics of rough surfaces in tribology: multiple asperity contact. Tribology letters, 4(1), 1-35..

- [26] Borri-Brunetto, M., Chiaia, B., & Ciavarella, M. (2001). Incipient sliding of rough surfaces in contact: a multiscale numerical analysis. Computer methods in applied mechanics and engineering, 190(46), 6053-6073.

- [27] Conry, T. F., & Seireg, A. (1971). A mathematical programming method for design of elastic bodies in contact. Journal of Applied Mechanics, 38(2), 387-392..

- [28] Sahlin, F., Larsson, R., Almqvist, A., Lugt, P. M., & Marklund, P. (2010). A mixed lubrication model incorporating measured surface topography. Part 1: theory of flow factors. Proceedings of the Institution of Mechanical Engineers, Part J: Journal of Engineering Tribology, 224(4), 335-351..

- [29] Ilincic, S., Vorlaufer, G., Fotiu, P. A., Vernes, A., & Franek, F. (2009). Combined finite element-boundary element method modelling of elastic multi-asperity contacts. Proceedings of the Institution of Mechanical Engineers, Part J: Journal of Engineering Tribology, 223(5), 767-776.

- [30] Kalker, J. J., & Van Randen, Y. (1972). A minimum principle for frictionless elastic contact with application to non-Hertzian half-space contact problems. Journal of engineering mathematics, 6(2), 193-206..

- [31] Lai, W. T., & Cheng, H. S. (1985). Computer simulation of elastic rough contacts. ASLE transactions, 28(2), 172-180..

- [32] Ren, N., & Lee, S. C. (1993). Contact simulation of three-dimensional rough surfaces using moving grid method. Journal of tribology, 115(4), 597-601..

- [33] Poon, C. Y., & Sayles, R. S. (1994). Numerical contact model of a smooth ball on an anisotropic rough surface. Journal of tribology, 116(2), 194-201..

- [34] Sellgren, U., Björklund, S., & Andersson, S. (2003). A finite element-based model of normal contact between rough surfaces. Wear, 254(11), 1180-1188..

- [35] Webster, M. N., & Sayles, R. S. (1986). A numerical model for the elastic frictionless contact of real rough surfaces. Journal of Tribology, 108(3), 314-320..

- [36] Tian, X., & Bhushan, B. (1996). A numerical three-dimensional model for the contact of rough surfaces by variational principle. Journal of tribology, 118(1), 33-42..

- [37] Aghdam, A. B., & Khonsari, M. M. (2011). On the correlation between wear and entropy in dry sliding contact. Wear, 270(11), 781-790.

- [38] Bryant, M. D., Khonsari, M. M., & Ling, F. F. (2008). On the thermodynamics of degradation. Proceedings of the Royal Society A: Mathematical, Physical and Engineering Science, 464(2096), 2001-2014..

- [39] Gershman, I. S., & Bushe, N. A. (2006). Elements of Thermodynamics of Self-Organization during Friction. Self-Organization during Friction. Advanced Surface-Engineered Materials and Systems Design, 13-58..

- [40] NADERI, M., AMIRI, M. & KHONSARI, M. (2010). On the thermodynamic entropy of fatigue fracture. Proceedings of the Royal Society A: Mathematical, Physical and Engineering Science, 466, 423-438.

- [41] NOSONOVSKY, M. (2010). Entropy in tribology: in the search for applications. Entropy, 12, 1345-1390.

- [42] PRIGOGINE, I. (1967). Introduction to thermodynamics of irreversible processes. New York: Interscience, 1967, 3rd ed., 1.

- [43] BULGAREVICH, S., BOIKO, M., KOLESNIKOV, V. & KORETS, K. (2010). Population of transition states of triboactivated chemical processes. Journal of Friction and Wear, 31, 288-293.

- [44] BULGAREVICH, S., BOIKO, M., KOLESNIKOV, V. & FEIZOVA, V. (2011). Thermodynamic and kinetic analyses of probable chemical reactions in the tribocontact zone and the effect of heavy pressure on evolution of adsorption processes. Journal of Friction and Wear, 32, 301-309.

- [45] Fujita, H., & Spikes, H. A. (2005). Study of zinc dialkyldithiophosphate antiwear film formation and removal processes, part ii: Kinetic model. Tribology transactions, 48(4), 567-575..

- [46] FUJITA, H. & SPIKES, H. (2004). The formation of zinc dithiophosphate antiwear films. Proceedings of the Institution of Mechanical Engineers, Part J: Journal of Engineering Tribology, 218, 265-278.

- [47] Mosey, N. J., Woo, T. K., Kasrai, M., Norton, P. R., Bancroft, G. M., & Müser, M. H. (2006). Interpretation of experiments on ZDDP anti-wear films through pressure-induced cross-linking. Tribology Letters, 24(2), 105-114..

- [48] DEMMOU, K., BEC, S., LOUBET, J.-L. & MARTIN, J.-M. (2006). Temperature effects on mechanical properties of zinc dithiophosphate tribofilms. Tribology international, 39, 1558-1563.

- [49] BOSMAN, R. & SCHIPPER, D. J. (2011). Running-in of systems protected by additive-rich oils. Tribology Letters, 41, 263-282.

- [50] ARCHARD, J. (1953). Contact and rubbing of flat surfaces. Journal of applied physics, 24, 981-988.

- [51] Suárez, Aldara Naveira. The Behaviour of Antiwear Additives in Lubricated Rolling-Sliding Contacts. Luleå University of Technology, 2011.

- [52] Podra, P., & Andersson, S. (1999). Simulating sliding wear with finite element method. Tribology International, 32(2), 71-81..

- [53] Hegadekatte, V., Kurzenhäuser, S., Huber, N., & Kraft, O. (2008). A predictive modeling scheme for wear in tribometers. Tribology International, 41(11), 1020-1031..

- [54] So, H., & Lin, Y. C. (1994). The theory of antiwear for ZDDP at elevated temperature in boundary lubrication condition. Wear, 177(2), 105-115.,

- [55] Willner, K. (2008). Fully coupled frictional contact using elastic halfspace theory. Journal of Tribology, 130(3), 031405..

- [56] KUZHAROV, A., BULGAREVICH, S., BURLAKOVA, V., KUZHAROV, A. & AKIMOVA, E. (2007). Molecular mechanisms of self-organization at friction. Part VI. Analysis of thermodynamic features of tribochemical reactions. Journal of Friction and Wear, 28, 218-223.

- [57] Fischer, T. E. (1988). Tribochemistry. Annual Review of Materials Science, 18(1), 303-323.

- [58] Spikes, H. (2004). The history and mechanisms of ZDDP. Tribology Letters, 17(3), 469-489.

- [59] Lin, Y. C., & So, H. (2004). Limitations on use of ZDDP as an antiwear additive in boundary lubrication. Tribology International, 37(1), 25-33.

Appendix 1

The elements of the coefficient matrix can be obtained using the full solution of the Boussinesq. The discretised form of the solution can be gained by integrating over the small rectangular area of 2a×2b as follow:

$$C^{zz} = \frac{1-\nu}{2\pi G}\left\{(x+a)\ln\left[\frac{(y+b)+\sqrt{(y+b)^2+(x+a)^2}}{(y-b)+\sqrt{(y-b)^2+(x+a)^2}}\right]\right.$$
$$+(y+b)\ln\left[\frac{(x+a)+\sqrt{(y+b)^2+(x+a)^2}}{(x-a)+\sqrt{(y+b)^2+(x-a)^2}}\right]$$
$$+(x-a)\ln\left[\frac{(y-b)+\sqrt{(y-b)^2+(x-a)^2}}{(y+b)+\sqrt{(y+b)^2+(x-a)^2}}\right]$$
$$\left.+(y-b)\ln\left[\frac{(x-a)+\sqrt{(y-b)^2+(x-a)^2}}{(x+a)+\sqrt{(y-b)^2+(x+a)^2}}\right]\right\}$$

$$C^{yy} = \frac{1}{2\pi G}\left\{(x+a)\ln\left[\frac{(y+b)+\sqrt{(y+b)^2+(x+a)^2}}{(y-b)+\sqrt{(y-b)^2+(x+a)^2}}\right]+(1\right.$$
$$-\nu)(y+b)\ln\left[\frac{(x+a)+\sqrt{(y+b)^2+(x+a)^2}}{(x-a)+\sqrt{(y+b)^2+(x-a)^2}}\right]$$
$$+(x-a)\ln\left[\frac{(y-b)+\sqrt{(y-b)^2+(x-a)^2}}{(y+b)+\sqrt{(y+b)^2+(x-a)^2}}\right]+(1$$
$$\left.-\nu)(y-b)\ln\left[\frac{(x-a)+\sqrt{(y-b)^2+(x-a)^2}}{(x+a)+\sqrt{(y-b)^2+(x+a)^2}}\right]\right\}$$

$$C^{xx} = \frac{1}{2\pi G}\left\{(1-\nu)(x+a)\ln\left[\frac{(y+b)+\sqrt{(y+b)^2+(x+a)^2}}{(y-b)+\sqrt{(y-b)^2+(x+a)^2}}\right]\right.$$
$$+(y+b)\ln\left[\frac{(x+a)+\sqrt{(y+b)^2+(x+a)^2}}{(x-a)+\sqrt{(y+b)^2+(x-a)^2}}\right]+(1$$
$$-\nu)(x-a)\ln\left[\frac{(y-b)+\sqrt{(y-b)^2+(x-a)^2}}{(y+b)+\sqrt{(y+b)^2+(x-a)^2}}\right]$$
$$\left.+(y-b)\ln\left[\frac{(x-a)+\sqrt{(y-b)^2+(x-a)^2}}{(x+a)+\sqrt{(y-b)^2+(x+a)^2}}\right]\right\}$$

$$C^{zx} = \frac{1-2\nu}{4\pi G}\left\{(y+b)ln\left[\frac{\sqrt{(y+b)^2+(x+a)^2}}{\sqrt{(y+b)^2+(x-a)^2}}\right] + (y-b)ln\left[\frac{\sqrt{(y-b)^2+(x-a)^2}}{\sqrt{(y-b)^2+(x+a)^2}}\right] + (x + a)\left[\tan^{-1}\frac{y+b}{x+a} - \tan^{-1}\frac{y-b}{x+a}\right] + (x-a)\left[\tan^{-1}\frac{y-b}{x-a} - \tan^{-1}\frac{y+b}{x-a}\right]\right\}$$

$$C^{zy} = \frac{1-2\nu}{4\pi G}\left\{(x+a)ln\left[\frac{\sqrt{(y+b)^2+(x+a)^2}}{\sqrt{(y-b)^2+(x+a)^2}}\right] + (x-a)ln\left[\frac{\sqrt{(y-b)^2+(x-a)^2}}{\sqrt{(y+b)^2+(x-a)^2}}\right] + (y+b)\left[\tan^{-1}\frac{x+a}{y+b} - \tan^{-1}\frac{x-a}{y+b}\right] + (y-b)\left[\tan^{-1}\frac{x-a}{y-b} - \tan^{-1}\frac{x+a}{y-b}\right]\right\}$$

$$C^{xy} = \frac{\nu}{2\pi G}\left[\sqrt{(y-b)^2+(x+a)^2} - \sqrt{(y-b)^2+(x-a)^2} + \sqrt{(y+b)^2+(x-a)^2} - \sqrt{(y+b)^2+(x+a)^2}\right]$$

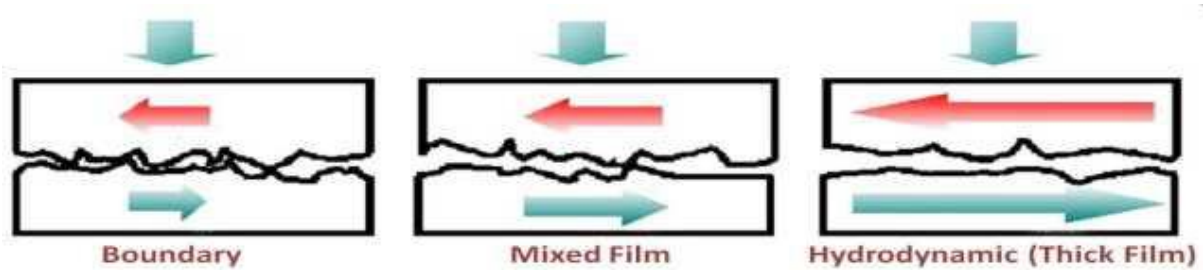

Figure 1 lubrication regimes

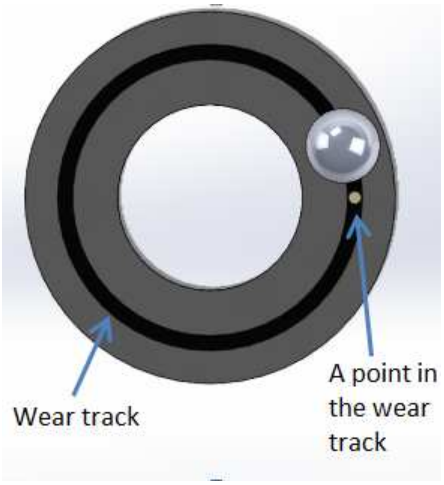

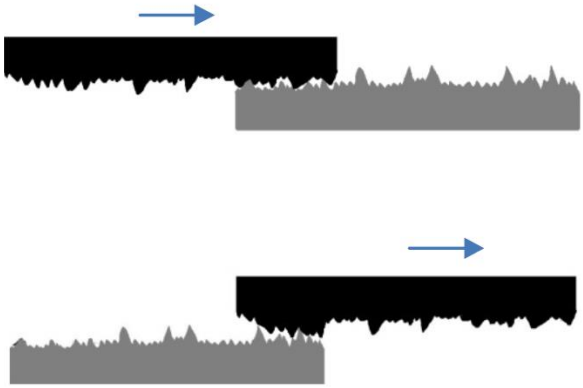

Figure 2 contact mechanics schematics

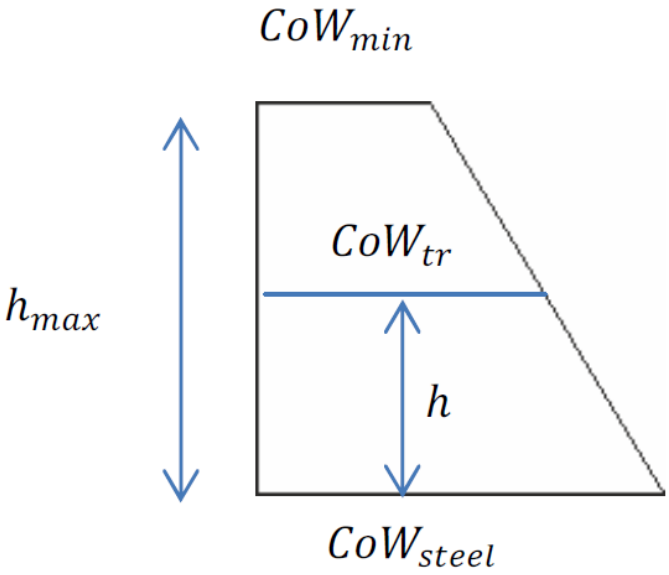

Figure 3 schematic of the proposed wear model

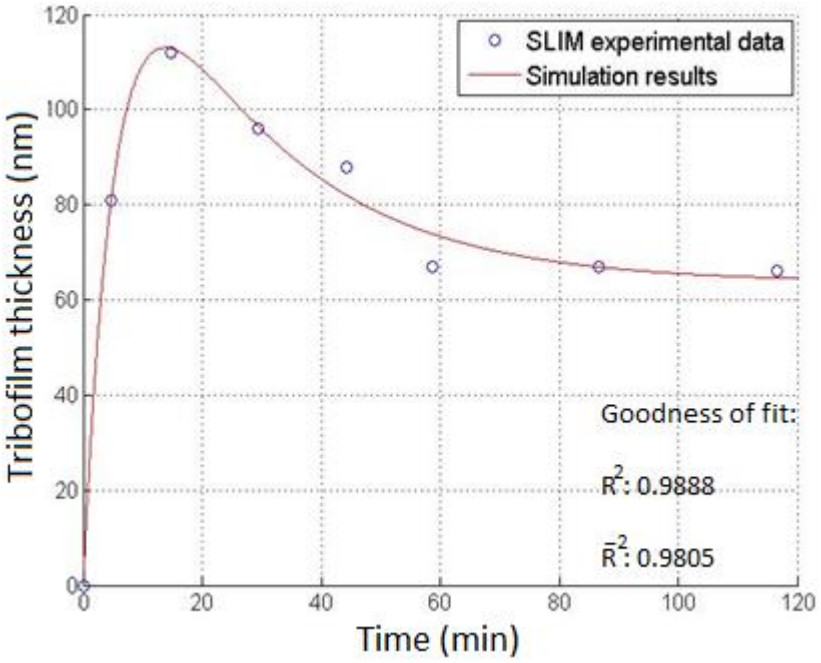

Figure 4 calibrated tribofilm growth results

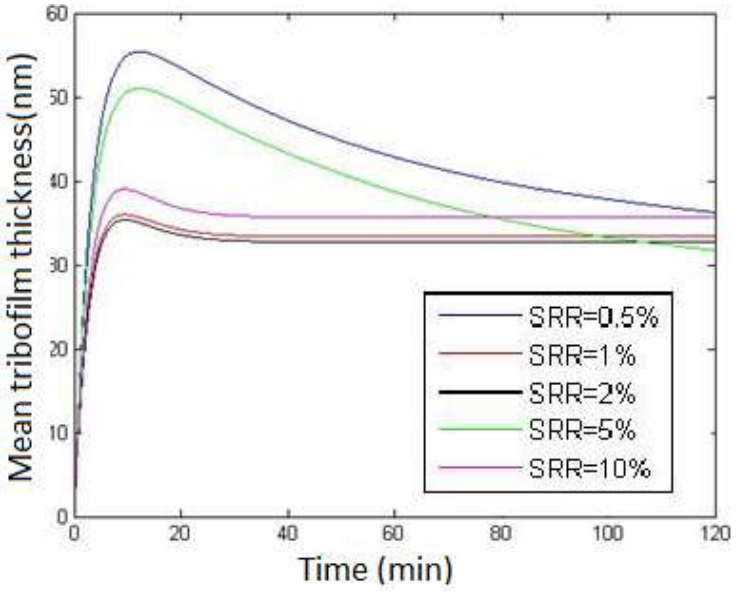

Figure 5 Average tribofilm thickness for different SRR

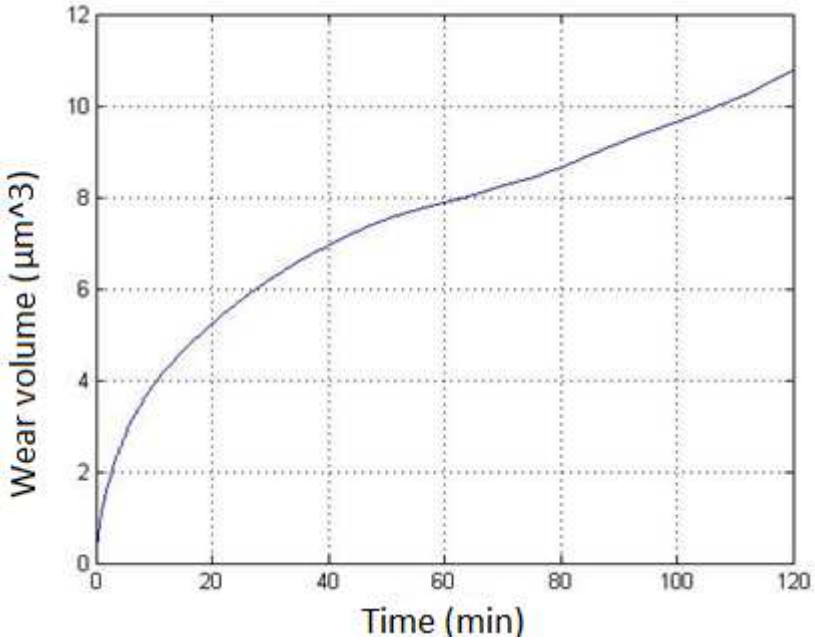

Figure 6 Wear calculation vs time

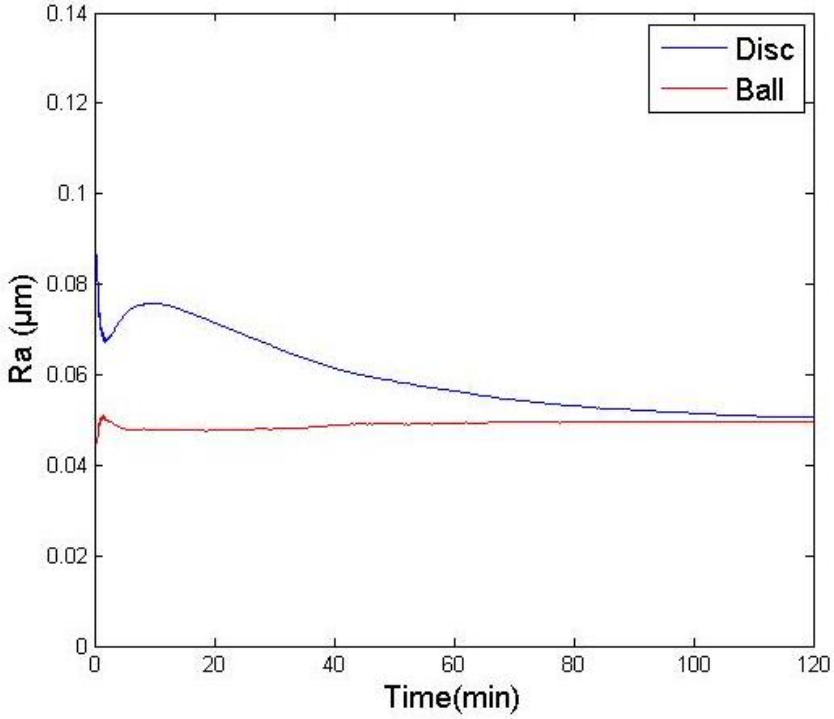

Figure 7 Ra value variations for two rubbing surfaces

Parameter	Value	Description
K or (COW_{steel})	10^{-5}	Dimensionless wear coefficient for steel
COW_{min}	10^{-6}	Dimensionless wear coefficient for maximum film thickness
h_{max}	176 nm	Maximum local tribofilm thickness in the formation process
x_{tribo}	4.13×10^{-16}	Tribofilm formation rate constant
C_1	0.1125	Tribofilm removal constant
C_2	0.0006799	Tribofilm removal exponential factor
E_1, E_2	210 GPa	Young's modulus of two surfaces
ν_1, ν_2	0.3	Poisson ratio
H_{steel}	6 GPa	Hardness of the steel substrate
H_{tr}	2 GPa	Hardness of the tribofilm at steady state tribofilm thickness
R^2	0.9888	Goodness of the fitting by R-Square
$\bar{R}^2$	0.9805	Goodness of the fitting by adjusted R-Square